

Hydrodynamics Modeling and Analysis Of Rapid Expansion Systems Of Supercritical Solutions (RESS)

Y. Samyudia*, F. Panau and Y.I. Liong

Department of Chemical Engineering
Curtin University of Technology, CDT 250, 98009 Miri, Sarawak, Malaysia

*Corresponding author. Ph: +60 85 443835; fax. +60 85 44 3837

Email: yudi.samyudia@curtin.edu.my

Abstract

In this paper, we study the hydrodynamics aspects of the RESS (e.g. rapid expansion of supercritical solutions) process to produce fine particles for heat-sensitive organic compounds. The Computational Fluid Dynamic (CFD) modeling and analysis of the supercritical solutions passing through a capillary nozzle were studied. The CFD simulation is focused on the pre-expansion chamber of the RESS process consisting of three successive steps that are at the stagnation chamber (i.e. the reservoir), nozzle inlet and along the nozzle itself to the outlet. The solute considered is benzoic acid and the supercritical solvents are CO₂ and CHF₃ respectively. The aim of this study is to examine the effect and sensitivity of the design parameters (i.e. temperature, pressure and density) on the formation of particulates in the chamber. The study reveals that at lower pre-expansion temperature with constant pre-expansion pressure the solute nucleation seems to start inside the nozzle. Moreover, it is also found that pre-expansion pressure has insignificant effect on the nucleation process, i.e. the nucleation rate slightly increases when the pressure is set higher. Furthermore, the study also reveals that high pre-expansion pressures and low pre-expansion temperature favors small particles. The results demonstrate that the variation of these parameters in the ranges studied may lead to the increased super-saturation and simultaneously increase in nucleation rate.

Keywords: RESS, Hydrodynamics; CFD Modeling; Particle formation

1. Introduction

Particle formation by methods utilizing supercritical fluids (e.g. CO₂) is a subject of great interests in many industrial applications such as pharmaceuticals, foods, natural products and specialty chemicals^[1,2,3,4]. Strict regulations on the use of organic solvents and their residual level in the end products form a major limitation to the traditional processing techniques. The particle formation using supercritical fluids (SCF) involves minimal or no use of organic solvents while the processing condition is relatively mild. Additionally, the SCF technology involves a growing of the particles in a controlled fashion to attain the desired morphology. This feature offers advantages as compared to some conventional techniques of particle size reduction (e.g. milling and grinding) so that the SCF-based particle formation is especially desirable for thermally sensitive materials.

The SCF technology for particle formation is rapidly evolving, as reflected by the number of modified processes reported since its inception^[5,6,7]. These include static supercritical fluid process (SSF), rapid expansion of supercritical solutions (RESS),

particle from gas-saturated solutions (PGSS), gas anti-solvent process (GAS), precipitation from compressed anti-solvent (PCA), aerosol solvent extraction system (ASES), supercritical anti-solvent process (SAS), and supercritical anti-solvent process with enhanced mass transfer (SAS-EM).

Previous studies have shown that the RESS process be one of the most promising techniques. The technique offers several advantages over conventional processes, which are either mechanical (crushing, grinding and milling), or equilibrium controlled (crystallization from solution). The RESS process can lead to very high super-saturation ratios, which leads to uniform conditions within the nucleation medium, and hence in principle to narrow particle size distributions and to form small particles. RESS can be used to precipitate mainly organic solutes upon expansion of a dilute solution from a supercritical or near critical solvent. This RESS concept can be implemented in relatively simple equipment, although particle collection from the gaseous stream is not easy.

The expansion step in RESS occurs through such a throttling device as an orifice, capillary tube or needle valve, which can support a large pressure drop without freezing. Changes in pressure, throttling device dimensions, concentrations of solute in the supercritical fluid and temperature cause wide variations in precipitate morphology (e.g. fibers to spheres). An increase in pre-expansion temperature under certain experimental conditions can lead to a transition of powder to fibrous morphology. Similarly, a decrease in pressure can also result in a powder to fiber morphology transition. This suggests that solutions with lower density are more likely to produce particles of a fibrous morphology in the RESS process. In addition to the dynamic variables of pressure, temperature and concentration, a fluid dynamic process variable – the geometry of the throttling device - has also been found to influence the morphology of the precipitate ^[8,9].

In this paper, we study the hydrodynamic behavior through a capillary nozzle in the RESS process using Computational Fluid Dynamics (CFD). The CFD simulation is focused on the pre-expansion chamber of the RESS process consisting of three successive steps. They are at the stagnation chamber (i.e. the reservoir), at the nozzle inlet and along the nozzle itself. The solute considered in this study is benzoic acid and the supercritical solvents are CO₂ and CHF₃ respectively. The study is aimed at identifying the effect and sensitivity of the design parameters (i.e. operating conditions such as pressure and temperature) in the pre-expansion path of the RESS process on the particulate formation. From the CFD simulation, it is found that high pre-expansion pressures and low pre-expansion temperature favor for the formation of small particles. Furthermore, for mixture of benzoic acid/carbon dioxide, the nucleation process inside the capillary nozzle could not be avoided. According to the classical nucleation theory, our analysis reveals that the lower nucleation rates should results in a delayed precipitation. Hence, it would be less time available for growth, resulting in smaller particles. The CFD modeling and analysis of RESS process provides information for understanding the basic trends that relate the particle formation with the expansion process conditions. It is therefore of important for optimization, control and design studies ^[10].

2. Modeling of the Capillary Nozzle in the RESS Process

In the Rapid Expansion of Supercritical Solution (RESS) process, the solutes are dissolved in a supercritical fluid through an extraction process from which the

supercritical solution is then rapidly expanded into a low temperature and pressure environment in the expansion unit. The sudden change in conditions leads to a large cooling rate, resulting in high super saturations with homogeneous nucleation and particle growth.

The expansion can take place across a capillary nozzle within a very short time (see Figure 1). The formation of particles from RESS process leads to the production of thin films, crystalline or amorphous powders with narrow and controllable particle size distribution, and intimate mixtures of amorphous materials.

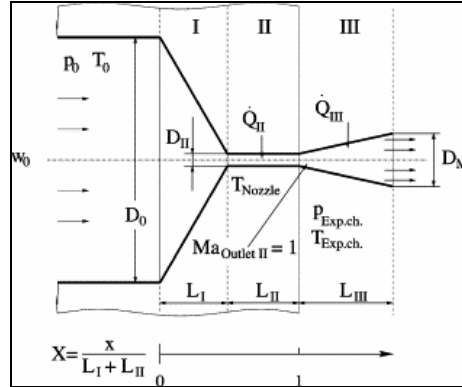


Figure 1. A schematic diagram of capillary nozzle in RESS

They are a number of process parameters that could influence the particle formation process when applying this RESS technology. They are the temperature and pressure in the pre expansion and post expansion chamber, the nozzle diameter and geometry, the solute and its concentration. Supercritical fluids are very dense gases with many properties superior to liquids or solvents. They combine properties of gases and liquids. The high compressibility of supercritical fluids leads to a fact that a small change in pressure can give a significant change in density that, in turn, affect diffusivity, viscosity, dielectric and salvation properties of these fluids, thus dramatically influencing the kinetics and mechanisms of chemical reaction.

The hydrodynamic model can be derived using the first principle of mass, momentum and energy balances, and the thermodynamic properties of the supercritical fluids were computed by means of the Bender equation of state as follows:

$$w \frac{d\rho}{dx} + \rho \frac{dw}{dx} + \frac{\rho w}{A} \frac{dA}{dx} = 0 \quad (1)$$

$$\rho w \frac{dw}{dx} + \frac{dp}{dx} = - \frac{2fw^2\rho}{D_{II}} \quad (2)$$

$$\frac{dh}{dx} + w \frac{dw}{dx} = \frac{dq}{dx} \quad (3)$$

$$P = RT\rho + B\rho^2 + C\rho^3 + D\rho^4 + E\rho^5 + F\rho^6 + (G + H\rho^2)\rho^3 e^{(-a_{20}\rho^2)} \quad (4)$$

Where w is the velocity, ρ the density, x the distance along the expansion device, A the flow area, f the Fanning friction factor, h the enthalpy and q the heat. P is the pressure (MPa), T is the temperature (K), and R is the universal constant for gases considered on a weight basis. The B, C, D, E, F, G, and H coefficients are defined by means of polynomial expressions that are temperature dependent and are correlated with the regression parameters. The proposed model of the expansion device is shown in Figure 1.

In this work, the hydrodynamic model for the RESS process is developed and implemented in CFD for a fixed geometry of the nozzle. Figure 2 and Table 1 shows a summary of the nozzle under study.

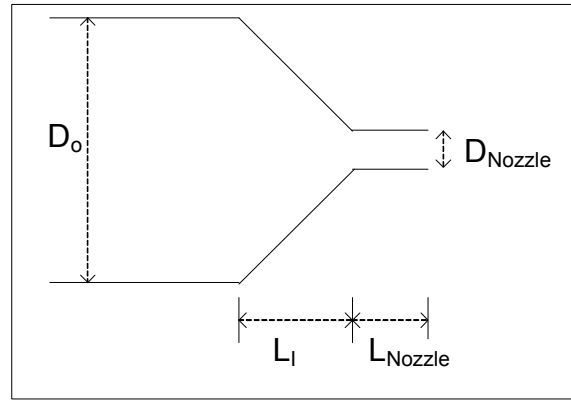


Figure 2: Schematic of capillary Nozzle for RESS Process

Table 1: Dimensions of the capillary Nozzle for RESS Process

Geometry	Dimensions in μm
Internal diameter D_o (μm)	1200
Diameter of capillary nozzle D_{Nozzle} (μm)	50
Length of inlet region L_I (μm)	330
Length of capillary nozzle L_{Nozzle} (μm)	50
Volume of the expansion chamber (dm^3)	22

The modeling objective is to study the effect and sensitivity of the design parameters (i.e. operating conditions) in the pre-expansion path of the RESS process on the particle formation in the chamber. Only simulation of the flow (i.e. hydrodynamic) in the capillary nozzle (capillary inlet – capillary nozzle) is carried out for the solvents of carbon dioxide (CO_2) and trifluoromethane (CHF_3) and for the organic solute of benzoic acid. The following assumptions were made on the flow inside the nozzle when developing and simulating the model:

1. The flow is steady and one-dimensional (i.e. flow along the axial direction)
2. The residence time inside the nozzle is very short

3. Adiabatic process is assumed so that no heat is transferred between the fluids inside the nozzle to the surrounding.
4. No phase change along the nozzle, one phase flow.

The boundary conditions are set as given in Table 2.

Table 2 Boundary conditions in CFD simulation

Boundary Type	Wall
Wall Influence On Flow	No Slip
Wall Roughness	Smooth Wall
Heat Transfer	Adiabatic
Boundary Type	Inlet
Flow Regime	Subsonic
Mass and Momentum	Static Pressure, 260bar
Flow direction	Zero Gradient
Turbulence	Zero Gradient
Heat Transfer	Static temperature, 383K
Boundary Type	Outlet
Flow Regime	Subsonic
Mass and Momentum	Static Pressure, 1 atm

The geometry of the nozzle is kept constant, only the pre-expansion temperature and pressure are changed. The outlet of the nozzle is kept at ambient condition. The sets of parameters are shown in Table 3.

Table 3: Sets of pre-expansion pressures and temperatures

Sets	Pre-expansion temperature (K)	Pre-expansion Pressure (MPa)
Set 1	383	26
Set 2	383	30
Set 3	418	26
Set 4	418	30

The CFX software package was used to simulate the nozzle expansion system. The heat transfer model and turbulence model are selected as the **total energy** and **k-epsilon models**. Heat transfer model are essentially used to predict the temperature throughout the flow. The types of heat transfer are via conduction, convection and also via turbulent mixing and viscous work. The **total energy** option to model the heat transfer was selected to model the transport of enthalpy, which includes kinetic energy

effects. This model is used for gas flows where the Mach number exceeds 0.2, and high-speed liquid flows where viscous heating effects arise in the boundary layer, in which the kinetic energy effects become significant. The flow inside the pre-expansion nozzle is approximately at supersonic condition which is consistent with the high-speed condition of the **total energy** model. In addition, the Turbulent Wall functions were selected to deal with fine meshes (0.01).

3. Simulation Results and Discussions

3.1 Pressure and Temperature Profiles

Figure 3 shows the profiles of pressure, temperatures and velocity (in terms of Mach number) along the nozzle. The results are comparable with the experimental data gathered from literature. From the figure, it can be observed that the temperature remains relatively constant until it reaches the position- x at 75 mm. However, the pressure would experience a significant drop across the x -direction. Hence, condensation becomes the prevailing precipitation mechanism up to the capillary exit. Prior to the exit, the pressure and temperature would drop from which the nucleation would occur. From the inlet to the capillary nozzle, it can be observed that the Mach number increase exponentially until it reaches over the supersonic condition, where $Ma=1.8$ at the nozzle exit. At $Ma=1$, the speed of the fluid can approach to the speed of sound. However, from the simulation of 100mm nozzle, the Ma number obtained at the end of the nozzle is significantly larger than those portrayed at the literature. Hence, due to the high speed, rapid expansion of the supercritical solution through the nozzle can be observed.

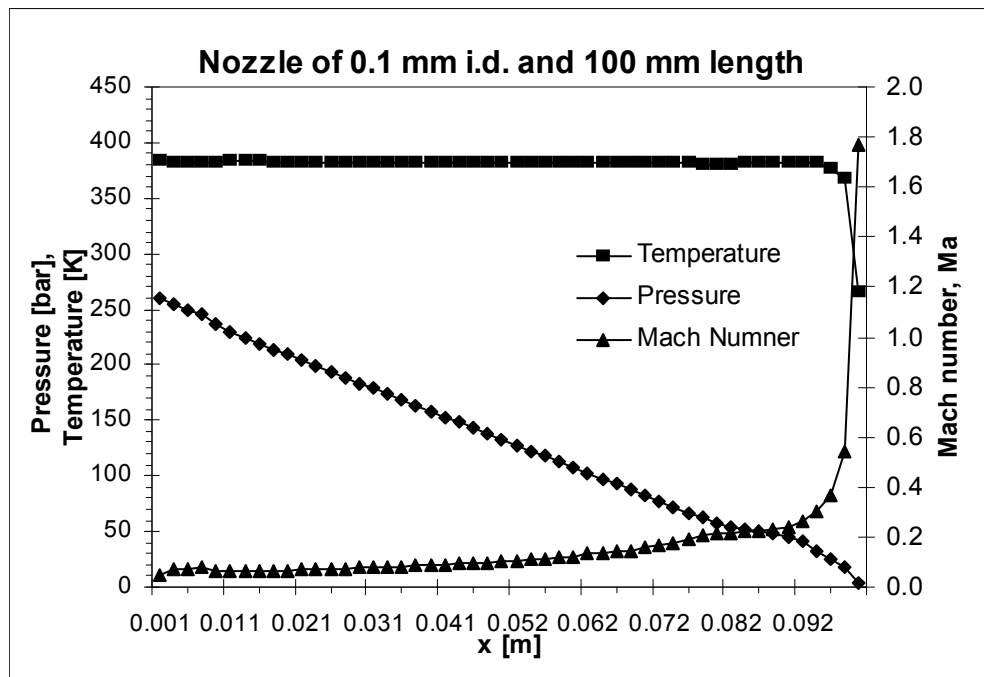


Figure 3: Profiles of pressure, temperature and Mach number along the nozzle.

3.2 Flow Profile Across the Nozzle

Figure 4 shows the profile of physical transport flow. It can be seen that the majority of bulk fluid (supercritical solutions) that enters the nozzle are from the peripheral region whereby at this region, the rate of deceleration of the flow is much lower because it is directed by the contracting wall and the friction force effect. Thus, this flow is more likely to enter the nozzle as it is more stable. Besides, there is a reduction in the probability of sudden languorous behavior as compared to the central bulk fluid where its surroundings are disordered medium itself. Hence the turbulent instability, eddies and vortices are likely to occur and slightly to shift the course of flow allowing a greater part of peripheral flow to enter.

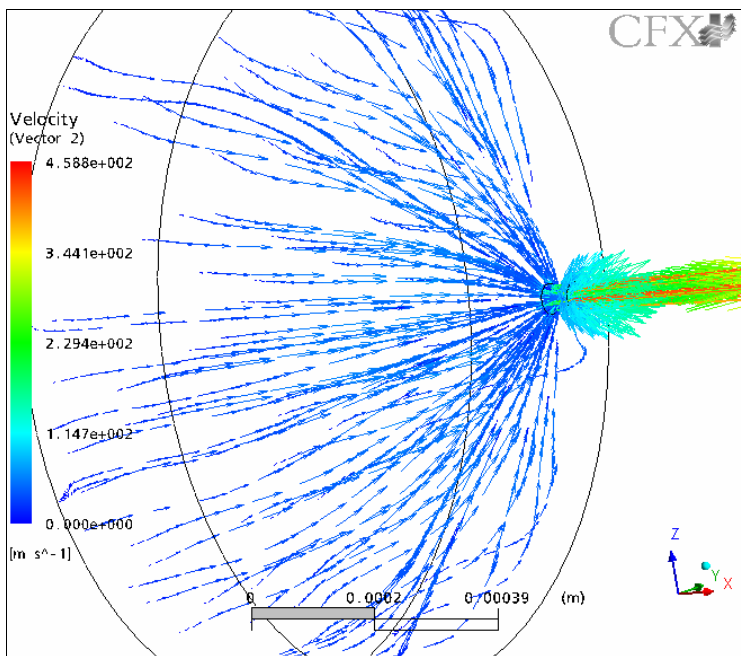


Figure 4: Flow profile across the nozzle.

3.3 Temperature Analysis

Figure 5 shows the temperature distribution of both supercritical solvents in pre-expansion. It can be seen that the temperature distribution for the reservoir region is not affected by the change in inlet pressure. Only a small deviation for both supercritical solvents because both solvents possess similarity in their properties where no effect of the pressure changes at higher temperature of 418K (SET 3 and SET 4) is observed. However, at lower inlet temperature of 383K, inlet pressure change will cause some significant effect on the temperature distribution. It is desirable to have a higher temperature distribution along the reservoir region because such high temperature increases its solubility.

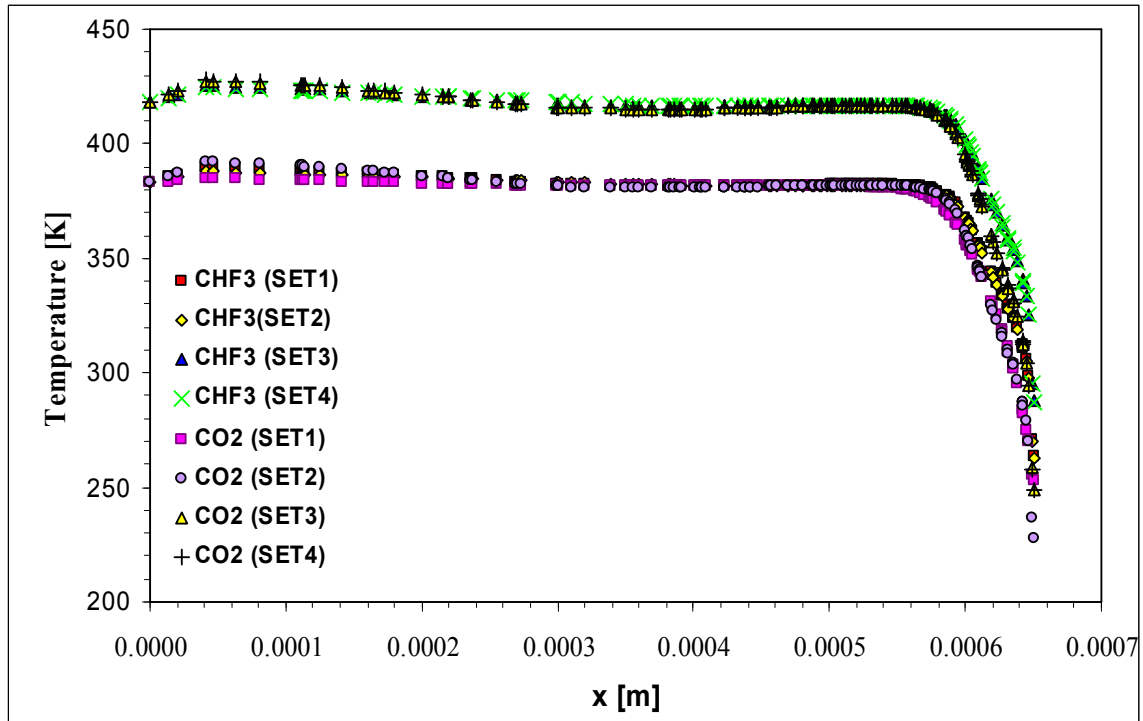


Figure 4: Central Temperature Distribution along Reservoirs and Nozzle for RESS

Figure 5 shows the temperature distribution at the nozzle region. From this figure, the higher temperature distribution is posed by CHF₃ as compared to CO₂ at similar condition. Therefore, one can infer that the rate of temperature decrement is much higher for CO₂ than CHF₃. By analyzing both Figures 4 and 5, we find that at higher constant inlet temperature or pressure, the differences in outlet temperature for CO₂ and CHF₃ increase from 18°C to approximately 40°C. Therefore, the discrepancy of solubility for both solvents will be more obvious when the inlet temperature increases. In addition, we observe from Figure 5 that for CO₂ the particle formation may take place earlier than that for CHF₃ because the temperature profile of CO₂ will intersect its critical boundary earlier than that of CHF₃ which implies that CO₂ solubility will decrease significantly.

3.4 Pressure Analysis

Figure 6 shows the pressure distribution for the RESS process. It is observed that the pressure gradient increases as it goes towards the nozzle with a huge degree of drop. This may be due to the rapid rise in velocity. Additionally, by looking at the trends for different supercritical solvents, increasing the inlet temperature from 383K to 418K at lower pressure of 26MPa (SET 1 & SET 3) will not affect the pressure distribution for CHF₃. In contrast, by varying the inlet temperature at higher pressure of 30MPa (SET 2 & SET 4), the pressure trends for CHF₃ will slightly diverge with the lower temperature inlet achieving a higher pressure as it approaches the nozzle. This is because at lower temperature, the viscosity of the solution will be slightly higher and therefore velocity is lower causing higher-pressure distribution. On the other hand for CO₂, the behavior is different whereby at higher pressure (30MPa), increasing the inlet temperature will not effect the pressure distribution while at lower pressure (26MPa), the temperature effect is

quite significant whereby the pressure distribution will remain constant for a longer period for the case of the lower inlet temperature. Furthermore, by comparing both solvents, one will be able to predict that pressure distribution for CHF₃ will always be slightly higher than CO₂ due to the change in velocity.

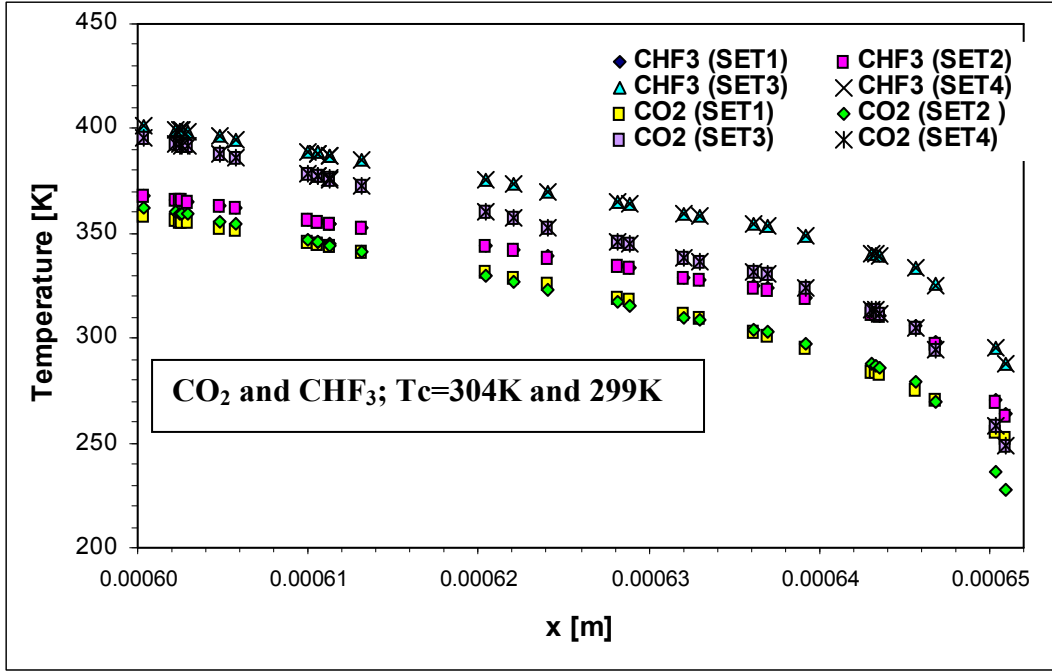


Figure 5: Central Temperature Distribution along Nozzle for RESS

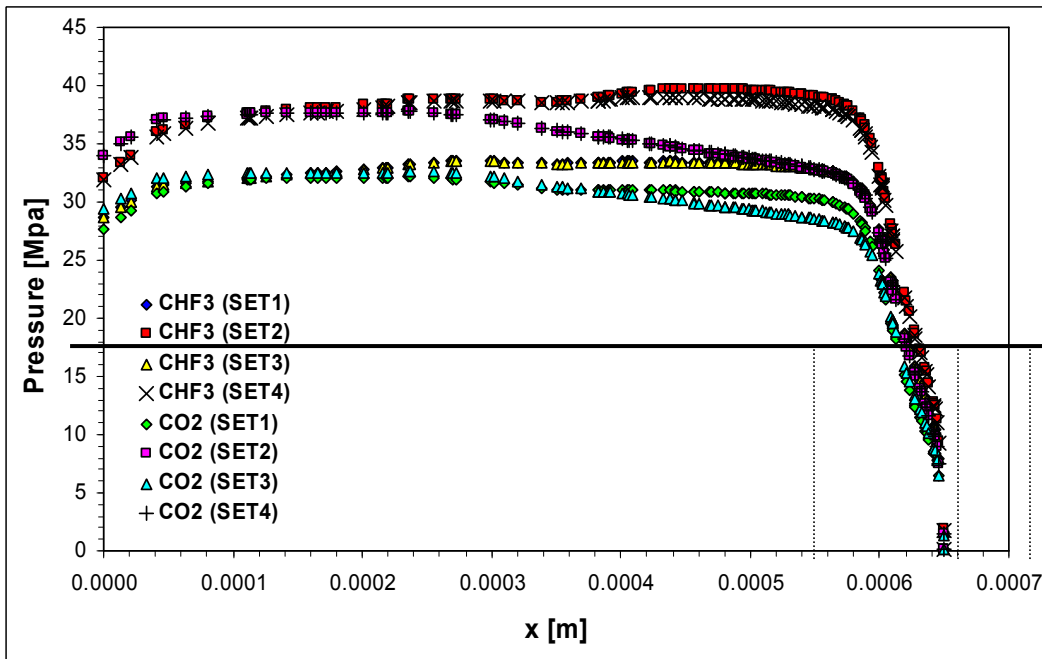


Figure 6: Central Pressure Distribution along Reservoirs and Nozzle for RESS

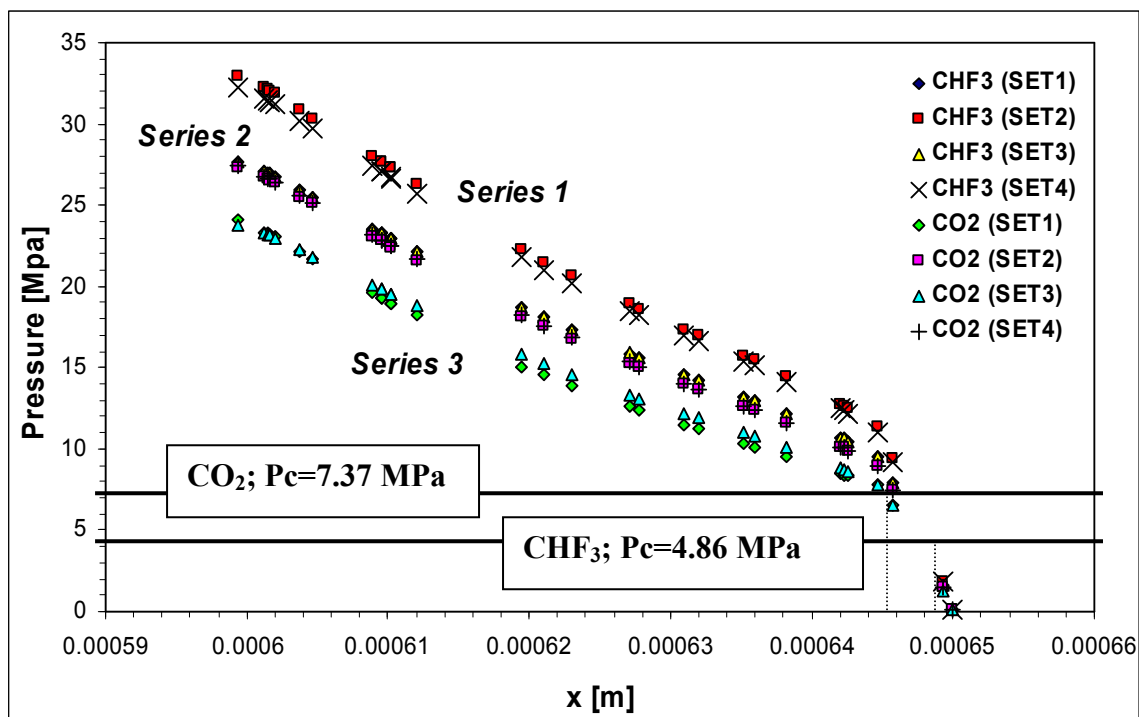


Figure 7: Central Pressure Distribution along Nozzle for RESS

Figure 7 shows the pressure distribution at the nozzle. From this Figure, it can be analyzed that the trends of pressure distribution for three series of data. Series 1 consists of SET 2 and SET 4 of CHF₃ with possessing highest-pressure distribution. As for Series 2, it composes of 4 sets and they are SET 1 and SET 3 of CHF₃ with SET 2 and SET 4 of CO₂. Hence, it can be analyzed that the effect of temperature and pressure to both supercritical solvents is contradictory to each other, i.e. the convergence of lower pressure distribution trend for CHF₃ and the higher-pressure distribution trend for CO₂. In addition, Figure 7 shows that the supercritical solvent of CO₂ reaches out of its critical region before CHF₃ does. Therefore, it can be predicted that the particle formation of benzoic acid can take place faster in CO₂ than CHF₃ due to the possibility of lost of solvent power. Likewise, from combined analysis of Figures 6 and 7, the relative pressure (P/P_c) for CO₂ is also much closer to 1 as compared to CHF₃.

3.5 Density Analysis

Figure 8 shows the density distribution along the pre expansion unit. Density is the most important parameter in the RESS process. If the density of the supercritical solvent is decreasing, the solvent power also decreases so that it leads to increase in supersaturation ratio.

It is desirable to attain the lowest density for a particular solvent at its supercritical region and at the nozzle exit because it increases the efficient use of supercritical solvent. Furthermore, the main purpose for the design parameter of pressure

and temperature is to alter and control the density and solvation power of the supercritical fluid so as to increase the performance of RESS process. At higher pressure, the density of the supercritical fluid (SCF) will increase due to compression of fluid to higher solidity. Conversely, at higher temperature, the density of SCF will drop as atoms in the fluid obtain higher thermal energy to pulsate from its usual position.

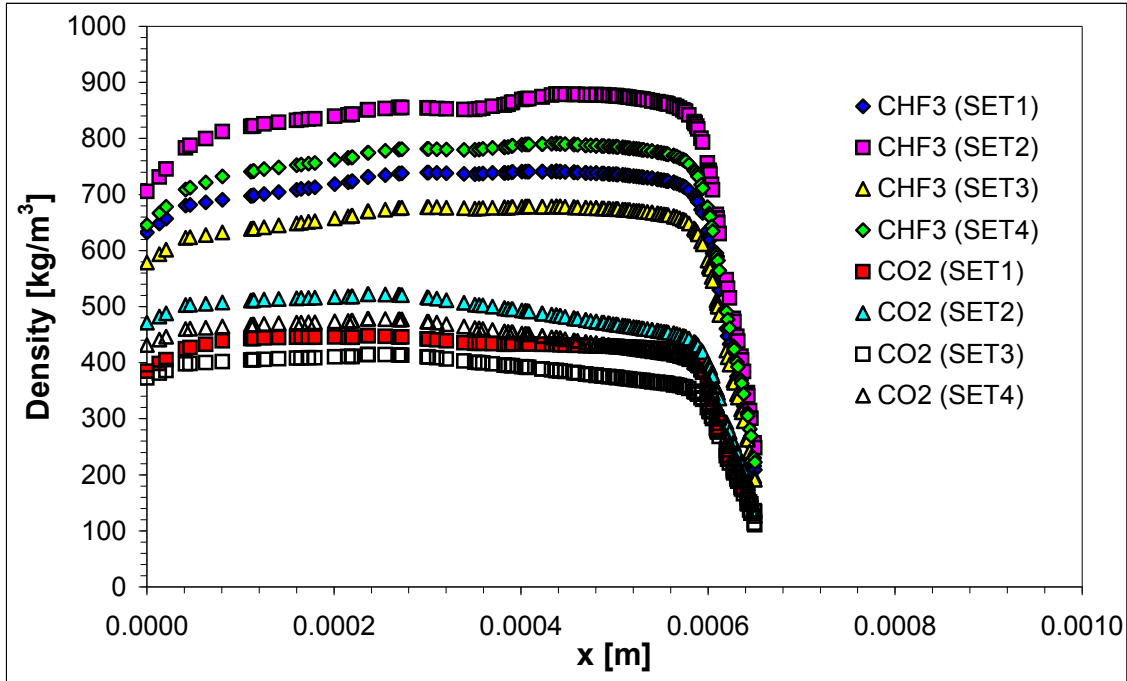


Figure 8: Central Density Distribution along Nozzle for RESS

Note that the compressibility factor should not be affected by the rate of dispersion of fluid jet or else depressurizing effect will be minimized and therefore deteriorate the RESS performance.

3.6 Discussions

Since high super saturation ratio is commonly used to calculate the critical nucleus radius, the high super saturation ratio corresponds to a low critical diameter. Moreover, a decrease in density means a decrease in solvent power. Consequently, this implies an increase in super-saturation power and the possibilities of increasing in the homogeneous nucleation rate.

From the simulation results, it is observed that at lower pre-expansion temperature with a constant pre-expansion pressure the solute nucleation may start inside the nozzle. This is due to the fact that the temperature of the fluid falls well below the critical points resulting in decreasing solvent power. In contrast, at higher pre-expansion temperature, the nucleation starts only at the nozzle outlet. This finding is true for both SCF of CO₂ and CHF₃.

It is also observed from simulation results that pre-expansion pressure slightly affects the nucleation process. Generally the nucleation rate is little higher when the pressure is higher. Thus, high pre-expansion pressures and low pre-expansion temperature favor small particle formation. High super-saturation rate tends to decrease the particle size.

4. Conclusions

Hydrodynamics modeling and analysis of RESS process has been presented in this paper. A CFD model has been developed for the specified nozzle from which the temperature, pressure and density profile analysis was conducted to condition the particle formation. The results demonstrate that the variation of these parameters in the ranges studied may lead to the increased super-saturation and simultaneously increase in nucleation rate.

Acknowledgment

This research was supported by Malaysian Pepper Board (MPB). The authors would like to thank MPB for the research grant.

References

1. Sitompul, J.P., I.N. Widiassa and Y. Samyudia, Prediction of Selectivity and Solubility of Ethanol in the Supercritical CO₂ Solvent, *Proc. of the National Seminar on Fundamental of Chemical Engineering, Institut Teknologi 10 November Surabaya*, 5-6 November 1997
2. Sitompul, J.P., Ratnawati, A. Suwono and Y. Samyudia, Solubility prediction of cholesterol in supercritical CO₂ involving cosolvent, *Proc. Of Int'l Conf. on Fluid Thermal and Energy Conversion, 21-24 July, Yogyakarta*, 207-214, 1997
3. Sitompul, J.P., A. Prasetyaningrum, T.H. Soeriawidjaja, Ratnawati, and Y. Samyudia, Extraction of β -carotene from its carrier by supercritical CO₂: Prediction of solubility and selectivity, *Proc. Of Int'l Conf. on Fluid Thermal and Energy Conversion, 21-24 July, Yogyakarta*, 257-264, 1997
4. Sitompul, J.P., I.N. Widiassa and Y. Samyudia, Combination of Powell's Dogleg and Hybrid Algorithms: Application to the Nonlinear Equation Systems of Phase Equilibrium on a Supercritical conditions (in Indonesian), *Proc. of the Seminar on Fundamental of Chemical Engineering, Institute of Technology 10 November, Surabaya*, 25-26 November, 1998
5. Tom, J.W. and P.G. Debenedetti, Particle formation with supercritical fluids – A review, *J. Aerosol Sci.*, 22 (5), 555-584, 1991
6. Türk, M., Formation of small organic particles by RESS: experimental and theoretical investigations, *J. of Supercritical Fluids*, 15, 79-89, 1999
7. Türk, M, B. Helfgen, P. Hils, R. Lietzow and K. Schaber, Micronization of pharmaceutical substances by rapid expansion of supercritical solutions (RESS): Experiments and Modeling, *Part.Part. Syst. Charact.*, 19, 327-335, 2002

8. Vemavarapu, C., M.J. Mollan, M. Lodaya and T.E. Needham, Design and process aspects of laboratory scale SCF particle formation systems, *Int. J. of Pharmaceutics*, 292, 1-16, 2005
9. Weber, M., L.M. Russell, and P.G. Debenedetti, Mathematical modeling of nucleation and growth of particles formed by the rapid expansion of a supercritical solution under subsonic conditions, *J. of Supercritical Fluids*, 23, 65-80, 2002
10. Samyudia, Y., P.L. Lee and I.T. Cameron, Control strategies for a supercritical fluid extraction process, *Chem. Eng. Science*, 51(5), 769-787, 1996